

A MATHEMATICAL MODEL OF THE NEWTONIAN FLUID FLOW IN THE PRESENCE OF APPLIED MAGNETIC FIELD

SUSHIL KUMAR JAIN, S. KUMAR and D.S. SHARMA

Department of Mathematics, St. John's College, Agra 282002, India

E-mail : Sushiljain002@gmail.com ; drdssharma.sjc@gmail.com.

Received : January 7, 2014

Abstract : Newtonian blood flow under the action of an applied magnetic field is proposed through this chapter which is a biomagnetic fluid dynamics (BFD) problem. As it is suitable for the description, it is consistent with the principles of ferrohydrodynamics and unlike magneto hydrodynamics takes into account. Both magnetization and electrical non-conductivity of blood is considered as a homogeneous Newtonian fluid. The laminar, incompressible, three-dimensional, fully developed viscous flow of a Newtonian biomagnetic fluid (blood) in a straight rectangular duct is studied under the action of a spatially varying magnetic field. The solution is then obtained by using a finite differences technique based on a pressure-linked pseudo transient method on a collocated grid. The flow is appreciably influenced by the application of the magnetic field and in particular by the strength and the magnetic field gradient. Results concerning the velocity and temperature field, and rate of heat transfer indicate that the presence of magnetic field appreciable influence the flow field.

Keywords: Biomegnetic fluid, viscous flow, Pseudo transient, collocatedgrid, magnetic field gradient, velocity and temperature field.

2010 Mathematics Subject Classification: 92C10, 92C35, 76Z05

1. Introduction

Biomagnetic fluid dynamics (BFD) is a relatively new area in fluid mechanics investigating the fluid dynamics of biological fluids in the presence of magnetic field. Numerous applications have been proposed in bioengineering and medical sciences, specially the development of magnetic devices for cell separation, magnetic wound or cancer tumor treatment causing magnetic hyperthermia etc. A biomagnetic fluid is exists in a living creature and its flow is influenced by the presence of a magnetic field. The most characteristic biomagnetic fluid is blood, which behaves as a magnetic fluid, due to the complex interaction of the intercellular protein, cell membrane and the hemoglobin, a form of iron oxides, which is present at a uniquely high concentration in the mature red blood cells, while its magnetic property is affected by factors such as the state of oxygenation. As far as the work in this direction is concerned, then Kafoussias and Williams [4] worked on an improved approximation technique to obtain numerical solution of a class of two-point boundary value similarity problems in fluid mechanics, while Takeuchi et al. [13] worked on the orientation of red blood cells in a high magnetic field, while Matsuki et al. [9] observed the experimental considerations on automatic cooling device using temperature sensitive magnetic field. Further Haik et al. [2] discussed about the development of magnetic device for cell separation, while Yamaoka and Miyazaki [16] discussed about the heat transfer enhancement in lithium annular flow under transverse magnetic field. Kumar and Diwakar [7] worked on a biomagnetic fluid dynamic model for the MHD Couette flow between two infinite horizontal parallel porous plates and observed that the main flow component decreases with the increase of Hartmann number and the velocity decreases with the increases of the injection suction parameter, they also investigate the effects of Hartmann number and suction parameter along with the velocity and temperature distribution.

Kelvin et al. [6] worked on a study of relationship between geometrical variation of atherosclerotic arteries and flow resistance. The blood flow assessment in the aortic heart valve based on magnetic resonance images using

optical flow analysis were discussed by Wong et al. [15]. Sankar and Hemalatha [11] worked on pulsatile flow of Herschel–Bulkley fluid through catheterized arteries, through a mathematical model. Misra et al. [10] studied a mathematical analysis of blood flow through an arterial segment with time dependent stenosis. Kumar and Dixit [8] discussed about the effect of porous parameter for the blood flow in a time dependent stenotic artery, while Sankar [12] worked on two-phase non-linear model for blood flow in asymmetric and axisymmetric stenosed arteries. This chapter is basically designed to observe the behavior of a biomagnetic fluid, which is exposed to magnetize is describing by the magnetization property (M). It is the measure of the how much the magnetic field is affecting the magnetic fluid and, in general, it is a function of the magnetic field intensity (H) and the temperature (T). It is also determined the biomagnetic fluid flow, is presented and relation are involve the dependence of the saturation magnetization (M) on the temperature (T) and the magnetic field intensity (H). In order to proceed to the numerical solution for this model are obtaining the numerical results are presented on graph which shows the flow is appreciably influenced by the magnetic field.

2. Mathematical formulation

As the blood flows under the influence of a magnetic field, two major forces will act upon it. The first one is the magnetization force due to the tendency of the erythrocytes to orient with the magnetic field and the second one is the Lorentz force arises due to the electric current generating from the moving ions in the plasma which is negligible.

The mathematical model for the BFD is based on the modified Stokes principles and on the assumption that besides the three thermodynamic variables, e.g. pressure (P), density (ρ) and temperature (T), the biomagnetic fluid behavior depends on the magnetization (M), which is a measure of the effect of the magnetic field on the magnetic fluid. According to the above mentioned considerations the governing equations of flow for an incompressible, homogeneous, Newtonian biofluid are:

$$\nabla \cdot \bar{u} = 0 \quad \dots (1)$$

$$\frac{D\bar{u}}{Dt} = -\frac{1}{\rho} \nabla \cdot \bar{P} + \bar{F} + \nu \nabla^2 \bar{u} + \frac{\mu_0 M}{\rho} \nabla \cdot \mathbf{H} \quad \dots (2)$$

$$\nabla \times \mathbf{H} = \mathbf{J} = 0 \quad \dots (3)$$

$$\nabla \cdot \mathbf{B} = \nabla \cdot (\mathbf{H} + \mathbf{M}) = 0 \quad \dots (4)$$

$$\rho C_p \frac{DT}{Dt} + \mu_0 T \frac{\partial M}{\partial T} [\bar{\nabla} \cdot (\bar{\nabla} \mathbf{H})] = K \nabla^2 T + \eta \phi \quad \dots (5)$$

In the above equations ρ is the fluid density, P is the pressure, F is the body force per unit volume, μ is the dynamical viscosity, μ_0 is the magnetic permeability of vacuum, M is the magnetization, H is the magnetic field intensity, B is the magnetic induction, T is the temperature, k is the coefficient of thermal conductivity of the fluid, K is the coefficient of thermal conductivity of the fluid, C_p is the specific heat at constant pressure and ϕ is the dissipation function which has the following form:

$$\phi = 2 \left[\left(\frac{\partial u}{\partial x} \right)^2 + \left(\frac{\partial v}{\partial y} \right)^2 + \left(\frac{\partial w}{\partial z} \right)^2 \right] + \left(\frac{\partial v}{\partial x} + \frac{\partial u}{\partial y} \right)^2 + \left(\frac{\partial w}{\partial y} + \frac{\partial v}{\partial z} \right)^2 + \left(\frac{\partial u}{\partial z} + \frac{\partial w}{\partial x} \right)^2 - \frac{2}{3} \left(\frac{\partial u}{\partial x} + \frac{\partial v}{\partial y} + \frac{\partial w}{\partial z} \right)^2 \quad \dots (6)$$

The behavior of a biomagnetic fluid when it is exposed to magnetic field magnetized is described by the magnetization property. Magnetization (M) is the measure of how much the magnetic field affects the magnetic fluid. In an equilibrium situation the magnetization property is generally determined by the fluid temperature, density and magnetic field intensity. Equations describing the dependence of magnetization (M) on these quantities may be expressed as (if χ is a constant called magnetic susceptibility):

$$M = \chi H \quad \dots (7)$$

If K is a constant called paramagnetic coefficient and T is the Curie temperature, (although the Curie temperature of the biofluid does not subjected to magnetization) then following relation is given by Andersson and Valnes [1]:

$$M = K(T_c - T) \quad \dots (8)$$

If β is the critical exponent for the spontaneous or saturation magnetization (for iron $\beta=0.368$, $M_1=54$ Oe and $T_1=1.45$ K) then another equation for magnetization, below the Curie temperature T_c is discussed by Matsuki et al. [9].

$$M = M_1 \left(\frac{T_c - T}{T_1} \right)^\beta, \quad \dots (9)$$

Another equation involving the magnetic intensity (H) and the temperature (T) is given by Tzirtzilakis et al. [14]:

$$M = K_1 H \{T_c - T\}, \quad \dots (10)$$

where K_1 is constant.

Now if m is the particle magnetization, N is the number of particles per unit volume and k the Boltzmann's constant then the magnetization process of red blood cells behaves like the following function, which also describes the variation of magnetization for a magnetic fluid (Higashi et al. [13]):

$$M = mN \left[\coth \left(\frac{\mu_0 m H}{kT} \right) - \frac{kT}{\mu_0 m H} \right], \quad \dots (11)$$

3. Application

Consider an electrically non-conducting biomagnetic fluid in a impermeable rectangular duct of square cross-section of side (h). The flow is subjected to the action of an applied magnetic field of sufficient strength to saturate the biomagnetic fluid. The magnetic field is generated by an electric current going through a thin wire placed parallel to the axis of symmetry of the bottom plane of the duct.

The mathematical model for the biomagnetic fluid dynamics is based on the modified Stokes principles and on the assumption that besides the three thermodynamic variables, (pressure p , density ρ and temperature T), the biomagnetic fluid behavior is also a function of magnetization (M). A linear equation involving the magnetic intensity (H) and temperature (T) and the magnetization M_0 is given in $M_0 = K H (T_c - T)$ where T_c is the Curie

temperature and K is a constant quantity. Although, when the difference between temperatures is negligible then $M_0 = K H_0$, where H_0 is the magnetic field strength at the point $(0, 0)$.

Consider flow in three dimensions over a rectangular duct obeying the following equations in which at the fully developed flow, the velocity components $\bar{V} = (u, v, w)$ and the pressure p are governed by the mass conservation and the fluid momentum equation at the \bar{x}, \bar{y} and \bar{z} directions.

$$\bar{\nabla} \cdot \bar{V} = 0 \quad \dots (12)$$

$$\rho \frac{D\bar{V}}{Dt} = -\bar{\nabla}p + \eta \bar{\nabla}^2 \bar{V} + \mu_0 M \bar{\nabla}H \quad \dots (13)$$

where $\bar{H} = \sqrt{\bar{H}_x^2 + \bar{H}_y^2}$, with \bar{H}_x and \bar{H}_y are magnetic field intensity along the \bar{x} and \bar{y} co-ordinates respectively, and $\bar{H} = (\bar{H}_x, \bar{H}_y)$ may be represented by:

$$\bar{H}_x = \frac{\beta}{2\pi} \frac{\bar{x} - a}{(\bar{x} - a)^2 + (\bar{y} - b)^2} \quad \text{and} \quad \bar{H}_y = -\frac{\beta}{2\pi} \frac{\bar{y} - b}{(\bar{x} - a)^2 + (\bar{y} - b)^2} \quad \dots (14)$$

For the flow problem under consideration $a = h/2$ and $b = -c$. On the basis of above information may be consider the magnitude of the magnetic field intensity as \bar{H} and may be written as:

$$\bar{H}(\bar{x}, \bar{y}) = \left[\bar{H}_x^2 + \bar{H}_y^2 \right]^{1/2} = \frac{\beta}{2\pi} \frac{\bar{y} - b}{(\bar{x} - a)^2 + (\bar{y} - b)^2} \quad \dots (15)$$

where β is the magnetic field strength at the point $(\bar{x} = a, \bar{y} = b)$.

The boundary conditions are:

$$\bar{u} = 0 = \bar{v} = \bar{w} \quad \text{at} \quad \bar{y} = -h/2 \quad \text{or} \quad \bar{y} = h/2 \quad \text{and} \quad -h/2 \leq \bar{x} \leq h/2 \quad \dots (16)$$

$$\bar{u} = 0 = \bar{v} = \bar{w} \quad \text{at} \quad \bar{x} = -h/2 \quad \text{or} \quad \bar{x} = h/2 \quad \text{and} \quad -h/2 \leq \bar{y} \leq h/2 \quad \dots (17)$$

The last term of the equation (xii) represents the components of magnetic force per unit mass along the \bar{x} and \bar{y} co-ordinates, but $\frac{\partial \bar{H}}{\partial \bar{z}} = 0$.

4. Transformation of the basic equations

The following non-dimensional quantities, helps to make the basic equations in dimensionless form

$$x = \bar{x}h, \quad y = \bar{y}h, \quad z = \bar{z}h, \quad u = \frac{\bar{u}U}{h}, \quad v = \frac{\bar{v}U}{h}, \quad w = \frac{\bar{w}U}{h}, \quad p = \frac{\bar{p}\rho U^2}{h^2},$$

$$H = \bar{H}H_0, \quad t = \frac{\bar{t}\rho h^2}{\sigma_0} \quad \dots (18)$$

For the pressure, which is the function of x, y and z, we can brake into two parts as follows:

$$p = p_1(z) + p_2(x, y) \quad \dots (19)$$

so that $\frac{\partial p}{\partial z} = p_z = \text{constant}$ and $\frac{\partial p}{\partial x} = p_x, \frac{\partial p}{\partial y} = p_y$.

Using the above non-dimensional variable (18), the basic equation (12) to (17) may be expressed as:

$$\frac{\partial u}{\partial x} + \frac{\partial v}{\partial y} = 0 \quad \dots (20)$$

$$\frac{\partial u}{\partial t} + u \frac{\partial u}{\partial x} + v \frac{\partial u}{\partial y} = -\frac{\partial p}{\partial x} + \frac{\partial^2 u}{\partial x^2} + \frac{\partial^2 u}{\partial y^2} + M H \frac{\partial H}{\partial x} \quad \dots (21)$$

$$\frac{\partial v}{\partial t} + u \frac{\partial v}{\partial x} + v \frac{\partial v}{\partial y} = -\frac{\partial p}{\partial y} + \frac{\partial^2 v}{\partial x^2} + \frac{\partial^2 v}{\partial y^2} + M H \frac{\partial H}{\partial y} \quad \dots (22)$$

$$\frac{\partial w}{\partial t} + u \frac{\partial w}{\partial x} + v \frac{\partial w}{\partial y} = -p_z + \frac{\partial^2 w}{\partial x^2} + \frac{\partial^2 w}{\partial y^2} \quad \dots (23)$$

along with the boundary conditions become:

$$u = 0 = v = w \text{ at } y = -\frac{1}{2} \text{ or } y = \frac{1}{2} \text{ and } x \in [-.2, .2] \quad \dots (24)$$

$$u = 0 = v = w \text{ at } x = -\frac{1}{2} \text{ or } x = \frac{1}{2} \text{ and } y \in [-.2, .2] \quad \dots (25)$$

where magnetic number M is represented by $h^2 \sigma_0 K H_0^2 / (v^2 \rho)$.

The basic partial differential equations (20)-(23) and the boundary conditions (24)-(25), involve dimensionless parameters, are coupled non-linear system of

partial differential equation describing the biomagnetic fully developed fluid flow in a rectangular duct.

5. Numerical solution

An approximate solution based on the pressure-linked equation method (PLEM) is used to solve the system of partial differential equations (20)-(23) along with the boundary conditions (24)-(25). Here it is unpractical to use the very well-known vorticity-stream function formulation because the cross-derivative vanish pressure along with the term due to magnetic field.

Thus, we use the pressure-linked equation method (PLEM) scheme using to arranged orthogonal grid, for neglecting the intricacy complication of the discretized differential equations using a staggered grid. In a arrangement grid, all the variables determined at the same grid nodes whereas, in a staggered grid each variable is determined at different grid point, which is discussed by Kafoussias and Xenos [5]. The pressure-linked equation method allow following algorithm be generated from the system of equations (20)-(23). Let (u', v', w') be an approximate solution of the equations (20)-(25), computed numerically for a given value of the axial pressure gradient component p_z and approximate value of the pressure p^i , while the correction of the velocity component, and introduces the pressure correction p_c . Hence required variables are written as

$$u = u' + u_c, \quad v = v' + v_c, \quad p = p^i + p_c \quad \dots (26)$$

Now consider equation (21) which in terms of the estimated variable u' , v' and p^i takes the following form:

$$\frac{\partial u'}{\partial t} + u' \frac{\partial u}{\partial x} + v' \frac{\partial u'}{\partial y} = -\frac{\partial p^i}{\partial x} + \frac{\partial^2 u'}{\partial x^2} + \frac{\partial^2 u'}{\partial y^2} + M H \frac{\partial H}{\partial \bar{x}} \quad \dots (27)$$

Using (26) the difference of (27) with (21) is

$$\frac{\partial u_c}{\partial t} + u' \frac{\partial u_c}{\partial x} + v' \frac{\partial u_c}{\partial y} = -\frac{\partial p_c}{\partial x} + \frac{\partial^2 u_c}{\partial x^2} + \frac{\partial^2 u_c}{\partial y^2} \quad \dots (28)$$

Now the consideration of the terms $(v' \cdot \nabla)u_c$ and $\nabla^2 u_c$ increases substantially the complexity, therefore we can neglect these terms without affecting the accuracy. Hence neglecting the above terms from (28), it results.

$$\frac{\partial u_c}{\partial t} = -\frac{\partial p_c}{\partial x} \quad \dots (29)$$

We can also show that the time derivative use the forward difference and considering that $u_c=0$ at the time step (i). We conclude that at the time step $(i+1)$ the correction u_c will be given by:

$$u_c^{i+1} = -\Delta t \frac{\partial p_c}{\partial x} \quad \dots (30)$$

Similarly for the correction v_c :

$$v_c^{i+1} = -\Delta t \frac{\partial p_c}{\partial y} \quad \dots (31)$$

The continuity equation (20) has the value of u and v from equation (xxiv) at each time step, and taking into account (29) and (30) leads to the Poisson equation, for the pressure correction, of the form

$$\frac{\partial^2 p_c}{\partial x^2} + \frac{\partial^2 p_c}{\partial y^2} = \frac{1}{\Delta t} \left(\frac{\partial u'}{\partial x} + \frac{\partial v'}{\partial y} \right) \quad \dots (31a)$$

Now as per the boundary conditions for velocities, u', v' and w' at the wall, are zero. The boundary conditions for the pressure correction p_c are obtained from the values of (29) and (30) where $u_c = v_c = 0$ at the wall. Hence, the boundary condition are given by:

$$u' = 0 = v' = w' = p_{cy} \text{ at } y = -\frac{1}{2} \text{ or } y = \frac{1}{2} \text{ and } x \in [-.5, .5] \quad \dots (32)$$

$$u' = 0 = v' = w' = p_{cx} \text{ at } x = -\frac{1}{2} \text{ or } x = \frac{1}{2} \text{ and } y \in [-.5, .5] \quad \dots (33)$$

If the pressure gradient $p_z = \text{constant}$ is give any arbitrary negative value then it is necessary to give initial guesses ($t = 0$) at all the grid points of the computational domain and applying the pressure-linked equation method (PLEM) iteratively. The forces due to the affect of magnetic field are balance in the stagnant situation

of the fluid the transverse pressure gradient forces. Thus we start the iteration procedure at $i = 0$ and using, as initial guesses, zero velocities and the transverse

pressure gradients $P_y = MH\left(\frac{\partial H}{\partial x}\right)+10^{-12}$, $P_x = MH\left(\frac{\partial H}{\partial x}\right)+10^{-12}$ and

indicating that the fluid starts making in the transverse plane. Further we use Alternating Direction Implicit (ADI) method in which we will replace the value u' and v' into (21) and solving the equation with the SOR method, the pressure correction p_c is calculated.

We consider that the velocities w_c and v_c are also calculated from (19) and (20) thus, at each time level $(i+1)$ the required velocities and pressure, are now determined by the relation

$$u^{i+1} = u' + u_c, \quad v^{i+1} = v' + v_c, \quad w^{i+1} = w', \quad P^{i+1} = p^i + p_c \quad \dots (34)$$

We compare now both level $(i+1)$ and i at the time level. We find that difference between both level is less than a prescribed quantity ϵ , but the convergence principle does not hold. We set the new estimations level $(i + 1)$ as the level (i) ones and repeat the iteration procedure till we reach, to right accuracy.

6. Results

The above numerical technique is having a main advantage that, it is applicable to a common grid. Although, it observe that slightly oscillations still occur and the numerical results are not totally independent on the grid density. We observed that oscillations are increasing not only for relatively sparse grids but also with relatively dense ones.

Table 1: Residuals of the continuity and the u, v and w momentum equations, respectively, for various grids.

Grid	Rs c	Rs u	Rs v	Rs w	M
15x15	0.38×10^{-5}	0.48×10^{-3}	0.39×10^{-3}	0.36	0.0
15x15	0.19×10^{-1}	0.80×10^{-1}	0.85×10^{-1}	0.35	0.1×10^7
15x15	0.34×10^{-1}	0.69×10^{-1}	0.73×10^{-1}	0.36	0.2×10^7
15x15	0.40×10^{-1}	0.90×10^{-1}	0.93×10^{-1}	0.38	0.3×10^7
20x20	0.27×10^{-5}	0.25×10^{-3}	0.23×10^{-3}	0.56	0.0
20x20	0.32×10^{-5}	0.27×10^{-3}	0.25×10^{-3}	0.56	0.1×10^7
20x20	0.41×10^{-5}	0.37×10^{-3}	0.34×10^{-3}	0.56	0.2×10^7
20x20	0.71×10^{-5}	0.58×10^{-3}	0.60×10^{-3}	0.56	0.3×10^7
25x25	0.36×10^{-5}	0.76×10^{-3}	0.71×10^{-3}	0.09	0.0
25x25	0.42×10^{-2}	0.27×10^{-2}	0.25×10^{-2}	0.09	0.1×10^7
25x25	0.81×10^{-2}	0.40×10^{-2}	0.38×10^{-2}	0.09	0.2×10^7
25x25	0.10×10^{-1}	0.55×10^{-3}	0.73×10^{-3}	0.09	0.3×10^7

Let (u^*, v^*, w^*, p^*) the involved solution at all the grid points (i, j) of the computational domain, then the evaluated solution is substituted in the equation (21), although it will not give exactly zero at each (i, j) point but:

$$\frac{\partial u^*}{\partial t} + u^* \frac{\partial u^*}{\partial x} + v^* \frac{\partial u^*}{\partial y} + p_x^* - \frac{\partial^2 u^*}{\partial x^2} + \frac{\partial^2 u^*}{\partial y^2} - M H \frac{\partial H}{\partial x} = R_{i,j} \quad \dots (37)$$

The residual for this equation, $R_s u$, is defined as

$$R_s u = \frac{1}{mn} \sum_{i=1}^m \sum_{j=1}^n |R_{i,j}|$$

Similarly we can define the residuals for equations (18), (20) and (21) as $R_s c$ (Residual for continuity), $R_s v$ and $R_s w$, respectively.

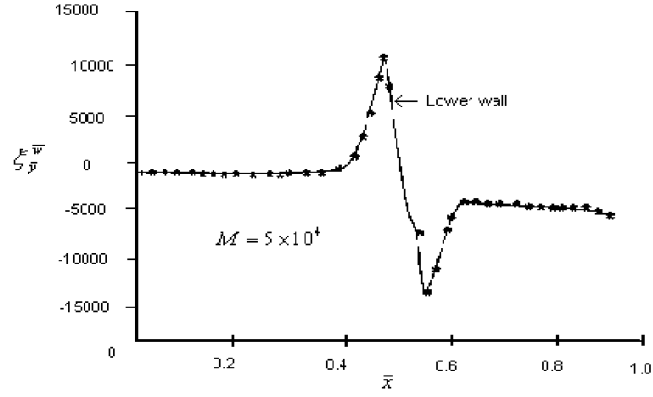


Figure 1. The variation of $\zeta_{\bar{y}}^{\bar{w}}$ on the lower wall with distance \bar{x}

If the τ_{yx} , τ_{yz} are force in the direction x and z respectively on a area perpendicular to y axis then this force (shear stresses) acting at the lower plane $PQQ'P'$, are defined as

$$\tau_{yx} = \sigma \left(\frac{\partial u}{\partial y} + \frac{\partial v}{\partial x} \right)_{y=0} = \left(\sigma \frac{\partial u}{\partial y} \right)_{y=0} = \left(\frac{\sigma v}{h^2} \frac{\partial u}{\partial y} \right)_{\bar{y}=0} \quad \dots (38)$$

Similarly
$$\tau_{yz} = \left(\frac{\sigma v}{h^2} \frac{\partial w}{\partial y} \right)_{y=0} \quad \dots (39)$$

At $PP'S'S$ (left plane) the acting stresses τ_{xy} and τ_{xz} are given by

$$\tau_{xy} = \left(\frac{\sigma v}{h^2} \frac{\partial v}{\partial x} \right)_{x=0} \quad \dots (40)$$

Similarly
$$\tau_{xz} = \left(\frac{\sigma v}{h^2} \frac{\partial v}{\partial x} \right)_{x=0} \quad \dots (41)$$

Calculate the following dimensionless quantities to obtain the stresses acting on the planes.

$$\frac{\partial u}{\partial y}_{y=0,1} = \zeta_y^u, \quad \frac{\partial v}{\partial x}_{x=0,1} = \eta_x^v, \quad \frac{\partial w}{\partial y}_{y=0,1} = \zeta_y^w \quad \text{and} \quad \frac{\partial w}{\partial y}_{x=0,1} = \zeta_x^w$$

We observe from the Fig. 1, that if, \bar{x} is increases then $\xi_{\bar{y}}^{\bar{w}}$ also increases taking its maximum positive value near to the place were the wire is located ($\bar{x}=0.48$). If \bar{x} is equal to 0.5 then $\xi_{\bar{y}}^{\bar{w}}$ is equal to zero and according to decreases taking its minimum negative value for $\bar{x}=0.52$. Now \bar{x} further increases tending to $\bar{x}=1$, $\xi_{\bar{y}}^{\bar{w}}$ is also increased taking asymptotic behavior of the results, its limiting value zero. The variation of $\xi_{\bar{y}}^{\bar{w}}$ with the dimensionless distance \bar{x} , for the lower wall (plane $PQQ'P'$, $\bar{y}=0$) and from $\bar{M}=5 \times 10^6$. We obtain that the variation of $\xi_{\bar{y}}^{\bar{w}}$ for the lower wall, is symmetrical with respect to the point $\bar{x}=0.5$, $\xi_{\bar{y}}^{\bar{w}}=0$.

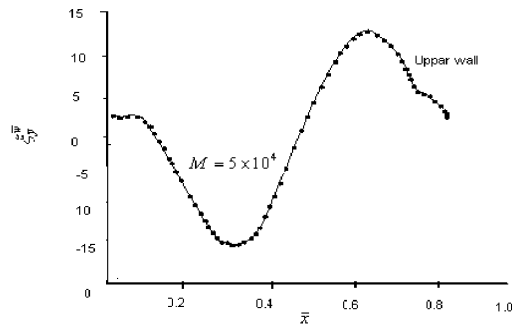


Figure 2. Variation of $\xi_{\bar{y}}^{\bar{w}}$ on the upper wall with distance \bar{x} .

Fig. 2 shows the behavior of $\xi_{\bar{y}}^{\bar{w}}$ for the upper wall, which is protected with respect to that of the lower plane. Although the variation in $\xi_{\bar{y}}^{\bar{w}}$ for the upper wall (plane $SRR'S'$, $\bar{y}=1$) is smooth and having a parabola character at each side of $\bar{x}=0.5$ and a magnitude of three order less than the corresponding one of the lower plane. This graph shows when \bar{x} increases from (0.0) to (0.3) then the variation of $\xi_{\bar{y}}^{\bar{w}}$ decreases and again when \bar{x} increases from (0.3) to (0.7) than the variation in $\xi_{\bar{y}}^{\bar{w}}$ increases. Therefore this process is depends upon the magnetic field strength, which decreases as the distance of \bar{y} increases from the wire position.

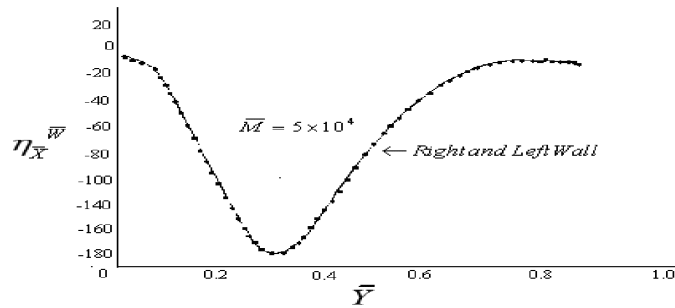


Fig. 3., Variation of $\eta_{\bar{x}}^{\bar{w}}$ on the left and right walls with distance \bar{y}

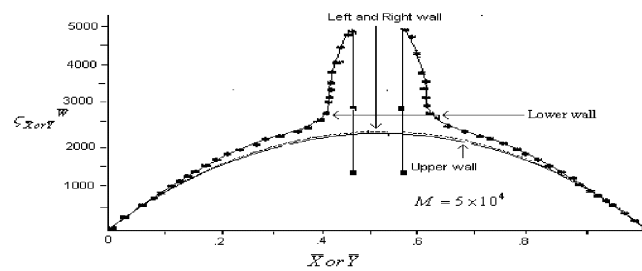


Fig. 4: Variation of $\zeta_{\bar{x} \text{ or } \bar{y}}^{\bar{w}}$ on all walls with the corresponding distance \bar{x} or \bar{y} .

The variation of $\eta_{\bar{x}}^{\bar{w}}$, with respect to \bar{y} , for the right ($\bar{x} = 1$) and left wall ($\bar{x} = 0$) is shown through the Fig. 3. Because of the symmetry of the flow field varies in the same way for the right and left wall, it is negative for all $y \in [0, 3]$ and its minimum value occurs at $\bar{y} \approx 0.3$. Here both the quantities $\eta_{\bar{y}}^{\bar{w}}$ and $\eta_{\bar{x}}^{\bar{w}}$ are the function of \bar{x} and \bar{y} respectively. Fig. 4. shows the variation of $\zeta^{\bar{w}}$, $\zeta_{\bar{x} \text{ or } \bar{y}}^{\bar{w}}$ for both planes with respect to y or x . It is obtained that $\zeta^{\bar{w}}$ varies almost identically for all the planes except the lower one. We can see at the lower wall there is increase of $\zeta^{\bar{w}}(\zeta_{\bar{y}}^{\bar{w}})$ moving towards the point $\bar{x} = 0.5$. Although a rapid decrement in the values of $\zeta^{\bar{w}}$ takes place close to $x = 0.5$ and within the interval $[0.46, 0.54]$ and the minimum value occurs exactly on $x = 0.5$.

Here observed that two vortices where risen at transverse plane, where as the axial velocity reduced. These conclusions suggest that a careful choice of the imposed magnetic field will affect the flow characteristics and hence can be utilized for possible medical and engineering applications. An application of the magnetic field affects considerably the flow field as well as the shear stresses, especially close to the area of the magnetic pole.

7. Conclusion

This phenomenon is extended, especially close to the source of the magnetic field, as the magnetic field strength increases, and we are also calculating the shear stresses acting on the wall of the channel. It was found that the magnetic field considerably influence these stresses, especially those acting on the lower plane near which is the source of magnetic field, the existence and the uniqueness of solution, obtained by the ADI method is ensured only for some of the difference equations. Again this chapter will also help for the further research in blood flow problems having the impact of magnetization.

References

- [1] Andersson, H. I. and Valnes, O. A. (1998). Flow of a heated ferrofluid over a stretching sheet in the presence of a magnetic dipole, *Acta Mech.*, **2**, 128-139
- [2] Haik, Y., Pai, V. and Chen C.J. (1999). Development of magnetic device for cell separation, *J. Magnetism and Magnetic Materials*, **194**, 254-261.
- [3] Higashi, T., Yamasishi, A., Takeuchi, T., Kawaguchi, N., Sagawa, S., Onishi, S. and Date M. (1993). Orientation of erythrocytes in a strong static Magnetic field, *Journal of Blood*, **82**, 1328-1334.
- [4] Kafoussias, N.G. and Williams, E.W. (1993). An improved approximation technique to obtain numerical solution of a class of two point boundary value similarity problems in fluid mechanics, *Int. J. Num. Method in Fluids*, **17**, 145-162.
- [5] Kafoussias, N.G. and Xenos, M.A. (2000). Numerical integration of two-dimensional turbulent boundary layer compressible flow with adverse pressure gradient and heat and mass transfer, *Acta Mech.* **141(3)**, 201-223.

- [6] Kelvin, K. L., Mazumdar, J. and Abbott, D. (2005). *A study of relationship between geometrical variation of atherosclerotic arteries and flow resistance*, Proc. 12th Int. Conf. on Biomedical Engineering, Singapore.
- [7] Kumar, S. and Diwakar, C.S. (2012). A mathematical model for Newtonian blood flow in the presence of applied magnetic field, *Aryabhatta J. of Math & Informatics*, **4**, 265-278.
- [8] Kumar, S. and Dixit, A. (2009). Effect of porous parameter for the blood flow in a time dependent stenotic artery, *Indian J. of Biomechanics Special Issue (NCBM 7-8 March)*., 22-25
- [9] Matsuki, H., Yamasawa, K. and Murakami, K. (1977). Experimental considerations on automatic cooling device using temperature sensitive magnetic fluid, *IEEE Trans. Magn.*, **5**, 1133-1143.
- [10] Misra J. C., Adhikar S. D. and Shit G. C. (2008). Mathematical analysis of blood flow through an arterial segment with time dependent stenosis, *J. of Mathematical Modeling and Analysis*, **13**, 401-412.
- [11] Sankar, D. S. and Hemalatha, K. (2007) Pulsatile flow of Herschel-Bulkley fluid through catheterized arteries-A mathematical model, *Applied Mathematical Modeling*, **31(8)**, 1497-1517.
- [12] Sankar, D.S. (2011). Two-phase non-linear model for blood flow in asymmetric and axisymmetric stenosed arteries, *Int. J. of Non-Linear Mechanics*, **46(1)**, 296-305.
- [13] Takeuchi, T., Mizuno, T., Higashi, T., Yamagishi, A. and Date, M. (1995). Orientation of red blood cells in high magnetic field, *J. of Magnetism and Magnetic Materials*, **5**, 1462-1463.
- [14] Tzirtzilakis, E. E. and Kafoussias, N. (2003). Biomagnetic fluid flow over a stretching sheet with non linear temperature dependent magnetization *ZAMP*, **8**, 54-65.
- [15] Wong, K. L., Kuklik, P., Kelso, P. M., Worthley, S. G. and Mazumdar, J. (2006). Blood flow assessment in the aortic heart valve based on magnetic resonance images using optical flow analysis, *Proc. 15th Int. Conf. Mechanics in Med & Biol. (ICMMB)*, **15**, 74-76.
- [16] Yamaoka, N. U. N. and Miyazaki, K. (2001). Heat transfer enhancement in lithium annular flow under transverse magnetic field. *Int. J. Eng. Sci.*, **43**, 441-447.